University of Baghdad
College of Engineering
JE
JOURNAL OF ENGINEERING

Journal of Engineering

journal homepage: www.joe.uobaghdad.edu.iq

Volume 29 Number 8 August 2023

Comparative Analysis of H2 and H∞ Robust Control Design Approaches for Dynamic Control Systems

Anwer J. Ali[1], Hayder H. Abbas[2,*], Hassan Bevrani[3]

[1]Technical Institute of Sulaimani, Sulaimani Polytechnic, University Sulaimani, Iraq
[2]Chemical Engineering Department, Koya University, Erbil, Iraq
[3]Department of Electrical Engineering SMGRC, University of Kurdistan, Sanandaj, Iran
anwer.ali@spu.edu.iq[1], hayder.hassan@koyauniversity.org[2], bevrani@uok.ac.ir[3]

ABSTRACT

This paper discusses using H2 and H∞ robust control approaches for designing control systems. These approaches are applied to elementary control system designs, and their respective implementation and pros and cons are introduced. The H∞ control synthesis mainly enforces closed-loop stability, covering some physical constraints and limitations. While noise rejection and disturbance attenuation are more naturally expressed in performance optimization, which can represent the H_2 control synthesis problem. The paper also applies these two methodologies to multi-plant systems to study the stability and performance of the designed controllers. Simulation results show that the H2 controller tracks a desirable closed-loop performance, while the H∞ controller guarantees robust stability for the closed-loop system. The validation of the techniques is demonstrated through the robust and performance gamma index, where the H∞ controller achieved a robust gamma index of 0.8591, indicating good robustness and the H2 controller achieved a performance gamma index of 2.1972, indicating a desirable performance. The robust control toolbox of MATLAB is used for simulation purposes. Overall, the paper shows that selecting a suitable, robust control strategy is crucial for designing effective control systems, and the H2 and H∞ robust control approaches are viable options for achieving this goal.

Keywords: Robust Control, Uncertainties, H2, H∞.

*Corresponding author
Peer review under the responsibility of University of Baghdad.
https://doi.org/10.31026/j.eng.2023.08.01

Article received: 28/01/2023
Article accepted: 31/07/2023
Article published: 01/08/2023

تحليل مقارن لطرق تصميم التحكم القوي (H2 وH∞)لأنظمة التحكم الديناميكي

ئه نور جلال علي[1]، حيدر حسن عباس[2]،*، حسن بيوراني[3]

[1] الجامعة التقنية السليمانية، جامعة بوليتكنك سليمانية، سليمانية، العراق

[2] قسم الهندسة الكيمياوية، جامعة كوية، اربيل، العراق

[3] قسم الهندسة الكهربائية، جامعة كردستان، سنانداج، ايران

الخلاصة

في هذا البحث تم مناقشة استخدام طرق المتحكم المتين (H2 وH∞) لتصميم نظام متحكم ، تم استخدام هذا المتحكمين لتصميم متحكم متين يتكون من (H2 وH∞) وتم تطبيق المتحكمات المقترحة على عدة أنظمة وتم دراسة إيجابيات وسلبيات كل طريقة على حدة . اثبت المتحكم (H∞) من خلال النتائج إمكانية التحكم المتين بالأنظمة المتعددة وكذلك حقق الأداء الجيد مع تحقيق الاستقرارية في العمل . أن متحكم (H2) اثبت الامثلية في السيطرة على الأنظمة قيد الدراسة وتامين حالة التغذية العكسية مع ضمان التعامل مع متغيرات النظام. استخدام المتحكمان (H2 و H∞) في هذا العمل البحثي وتطبيقه على عدة أنظمة مازالت قيد الدراسة والتطوير حيث اثبت المتحكمان إمكانية التحكم وتحقيق الأهداف المطلوبة . من خلال نتائج المحكاة تم التأكد من أنظمة السيطرة التي تم بناها في هذا العمل البحثي من خلال قيمة (robustness gamma index) في حالة متحكم H∞ كانت مقدار (gamma index of 0.8591) مما يثبت ان المتحكم متين ، وكان مقدار (gamma index of 2.1972) مما يدل على ان النظام (H2) اقل متانة من المتحكم (H∞) في هذا العمل البحثي تم استخدام برنامج الماتلاب وخاصة حزمة المتحكم المتين. بشكل عام ، تُظهر الورقة أن اختيار استراتيجية تحكم مناسبة وقوية أمر بالغ الأهمية لتصميم أنظمة تحكم فعالة ، وأن استخدام المتحكم القويين (H2 و H∞) هي خيارات قابلة للتطبيق لتحقيق اهداف المتحمكم المطلوب.

الكلمات الرئيسية: متحكم متين، عدم اليقين، H∞ ، H2 .

1. INTRODUCTION

The basic feature of robust control is that it ensures that the feedback system achieves stability and works well, even if the controlled process has uncertain parameters or is affected by noise or disturbances in the measurement **(Petersen, 2009; Vasičkaninová and Bakošová, 2015)**. A robust design controller is an approach to control the uncertainties and system-changing. These controllers can be coupled with several control criteria, including places for pole position, worst-case frequency response values, transient response decay rate limitations, and boundaries for the two robust controllers, H∞ and H2 norms **(Mehta et al., 2023).**

It has been demonstrated that the H∞ optimization strategy, created in the last two decades and currently under investigation, is a reliable and effective way to design linear, time-invariant control systems **(Gu et al., 2005; Maccari et al., 2012)** and time-variant control systems**(Lee et al., 2014; Mahmood et al., 2014)**. H2 and H∞ robust control methods, combined with various optimization-based approaches like fuzzy logic **(Li et al., 2008)**, artificial intelligence **(Wang et al., 2017)**, genetic algorithms **(Araque et al., 2021)**, and neural networks **(Yaghi and Önder Efe, 2020)**, provide a diverse set of tools to design

efficient and adaptive control systems capable of handling uncertainties and disturbances effectively.

Many researchers have addressed and studied the UAV system; for instance, **(Ibraheem, 2019)** proposed an Anti-Disturbance Compensator to stabilize a 6-DoF quadrotor Unmanned Aerial Vehicle (UAV) system. The designed Control Scheme rejects the disturbances subjected to this system and eliminates the effect of the uncertainties that the quadrotor system exhibits. In **(Saud and Hasan, 2018),** the Integral Backstepping Controller (IBC) is designed and optimized for full control of rotational and translational dynamics of an unmanned Quadcopter (QC), To improve controller capability in the steady state against disturbances; an integral action is used with the BC. To determine the optimal values of the IBC parameters, Particle Swarm Optimization (PSO) is used. Many researchers employed the H∞ and H2 controllers in their research.

For instance, in **(Lee et al., 2021)**, a large-scale unmanned aerial vehicle (UAV) is studied, and a controller is proposed. A reliable H∞ decentralized tracking control strategy is suggested to address a non-mountable impractical design issue brought on by the centralized control's excessive processing complexity. In **(Jiang et al., 2022),** a robust constrained H∞ control method is created, considering the in-wheel active suspension system's control limitation and the sprung mass variation's effects. Since Zames first introduced the concept of H∞ control synthesis, the area has seen significant development. The approach offers many theoretical advantages, some of which are strong disturbance rejection, great stability, and many more, where the H2 norm is used as a performance index. They have been extensively utilized to address several theoretical and practical issues. H∞ loop shaping is one of the strategies commonly recognized among those reviewed in this research paper's literature for the best H∞ controller. This is because performance criteria may be included in the design stage as performance weights **(Bansal and Sharma, 2013)**. Robust controllers can provide better results using a methodical approach to choosing suitable fractional weights **(Jafar et al., 2016; Guessoum et al., 2019)**. They propose the H∞ and H2 control designs as robust controllers for two systems addressed by **(Aghaie and Amirifar, 2007; Bansal and Sharma, 2013; Jafar et al., 2016)**.

This work emphasized the validity of H∞ and H2 robustness indices via addressed research problems named UAV and suspension system. The mathematical modeling and state space equations are derived, and an automatic weight selection algorithm is used to design control systems for UAV and active suspension systems. All simulations and validations are done using the Robust Control Toolbox of MATLAB.

2. PRELIMINARIES

The robust closed-loop (CL) control system can be written as robust H∞ and H2 optimization problems in many ways. Therefore, it is very helpful to have a standard way of putting a problem that can be changed to fit any problem. This generic formulation is made possible by the general arrangement shown in **Fig. 1 (Aghaie and Amirifar, 2007; Sojoodi and Majd, 2010)**, where *P* and *K* are generalizations for plant and controller, respectively. The overall control goal is to reduce a specific transfer function (TF) norm from w to z, such as the H∞ norm. Thus, the issue with controller design is to track down a controller K, using the data in v, that provides a control signal u that offsets the impact of w on z, hence reducing the CL norm from w to z.

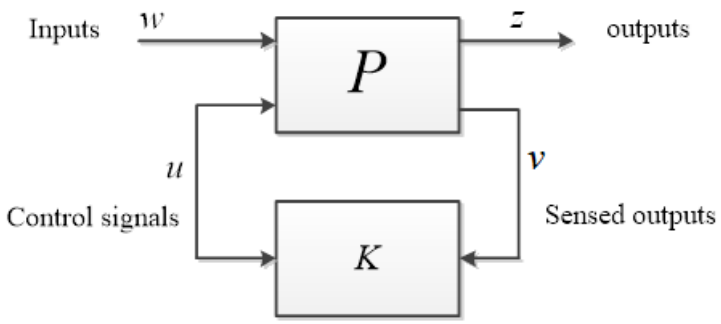

Figure 1. General Robust Control Problem.

$$\begin{bmatrix} z \\ v \end{bmatrix} = P(s)\begin{bmatrix} w \\ u \end{bmatrix} = \begin{bmatrix} P_{11}(s) & P_{12}(s) \\ P_{21}(s) & P_{22}(s) \end{bmatrix}\begin{bmatrix} w \\ u \end{bmatrix} \quad (1)$$
$$u = K(s)v$$

Eq. (1) represents a matrix of the robust control system, the w is the so-called external signals, such as disruptions and commands, and z is the "error" signals that must be reduced in some way to achieve the controller's design goals.

$$z = T_{zw}(s)w = F_l(P,K)w \quad (2)$$

where T_{wz} is the CL control system transfer matrix defined as:

$$T_{zw}(s) = F_l(P,K) = P_{11} + P_{12}K(I - P_{22}K)^{-1}P_{21} \quad (3)$$

H2 and H∞ control involve minimizing the H2 and H∞ norms of $F_l(P, K)$, respectively.

3. H∞ CONTROL

In the design of model-based controllers, system uncertainty is essential. A robust control method based on H∞ is suggested to address issues like amplifier delay and sensor offset, which are common examples of uncertainties that can be effectively mitigated using H∞ control **(Si et al., 2022)**. Robust control theory, which Zames first put out. When G (s) is the open TF of the plant P(s), and K(s) is the designed controller, this ensures the robustness and effective operation of the CL system. If the controller meets the following three criteria, controller $K(s)$ may be derived to allow the experiments to be repeated **(Vasičkaninová and Bakošová, 2015)**.

The stability of the system can be indicated through the roots of the characteristic equation (CE), which is the denominator of the TF; the roots should be placed on the left side of the complex s-Plane, and the sensitivity functions are kept small for all frequencies, and the performance criterion is met despite the large disturbances and operating point changes. Finally, the robustness criteria stipulate. Stability and performance must be maintained for the nominal and nearby plant models resulting from modeling errors. To provide high resilience of linear systems, robust controllers are built.

Typically, the highest value of a TF's H∞ norm, G, spanning the whole spectrum is denoted by:

$$\|G(j\omega)\|_\infty = sup\sigma G(j\omega) \quad (4)$$

Here, σ is defined as the largest singular value of a Tcontroller's goal to ensure constraint. Several controller design methods include the two- and three-TF approaches **(Bansal and Sharma, 2013)**. The former can be chosen over the latter for H controller synthesis since it has less computational complexity. A complicated control issue is traditionally split into two halves, one dealing with stability and the other with performance, using two transfer functions, which is the traditional method used in H∞ controller synthesis. The complementary sensitivity function, *T*, and the sensitivity function, *S*, provided in Eqs. (5) and (6) are necessary for the controller synthesis.

$$S = \frac{1}{1+P(s)K(s)} \quad (5)$$

$$T = \frac{P(s)K(s)}{1+P(s)K(s)} \quad (6)$$

Finding a controller *K* that minimizes the CL norm of *w* to *z* by generating a command signal *u* that opposes the impact of *w* on *z* based on the data in *v* . The values of *σ(S)* for performance and *σ(T)* for robustness can be constrained to achieve this, minimizing the norm **(Gu et al., 2005)**.

$$\min_K \left\| \begin{matrix} WsS \\ WtT \end{matrix} \right\|_\infty \quad (7)$$

W_s and W_t are called weighting functions that the designer indicates. These functions are sufficient to reduce the magnitudes of S and T to accomplish Eq. (8).

$$|S(j\omega)| < \frac{1}{Ws(j\omega)}, |T(j\omega)| < \frac{1}{Wt(j\omega)} \quad (8)$$

The size of the complementary sensitivity function is constrained by the robustness weighting function W_t, while the sensitivity function's size is constrained by the performance weighting function W_s, and control energy is constrained by the complementary sensitivity function W_{KS}. The loop shaping approach is the most popular method for selecting the weight functions for the controller's synthesis.

In general, the robust control design is constructed in such a way as to bring the H∞ norm of the plant down to its lowest possible value. To accomplish this condition and meet the state's requirements, three weight functions are introduced to the plant to shape the loop.

In their most fundamental form, weight functions are lead and lag compensators transfer functions that adjust the system's frequency response according to user preferences. Loop shaping is used with the WF to achieve the required frequency response from the plant. Loop shaping may be accomplished in several different ways. Adjusting the values of the weight functions' parameters is necessary to bring the entire system's frequency response within the acceptable range of values. **Fig. 2** shows the mixed Sensitivity problem addressed by **(Sojoodi and Majd, 2010; Vasičkaninová and Bakošová, 2015).**

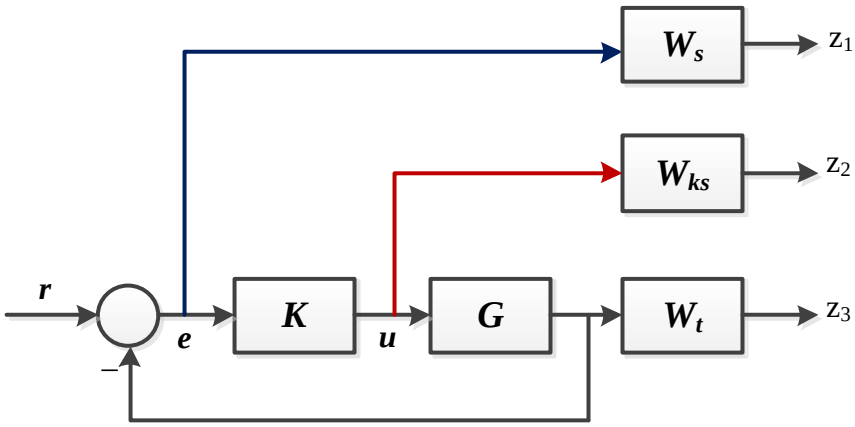

Figure 2. Synthesis model of plant controller.

The state-space equations that represent the generalized system *P* in **Fig. 1** are given in Eq. (9):

$$\begin{aligned} x(t) &= Ax(t) + B1w(t) + B2u(t) \\ x(t) &= Ax(t) + B1w(t) + B2u(t) \\ z(t) &= C1x(t) + D11w(t) + D12u(t) \\ y(t) &= C_2x(t) + D_{21}w(t) + D_{22}u(t) \\ y(t) &= C_2x(t) + D_{21}w(t) + D_{22}u(t) \end{aligned} \tag{9}$$

where $x(t) \in R^n$ is the state vector, $w(t) \in R^{m1}$ the exogenous input vector, $u(t) \in R^{m2}$ the control input vector, $z(t) \in R^{p1}$ the error (output) vector, and $y(t) \in R^{p2}$ the measurement vector, with $p1 \geq m2$ and $p2 \leq m1$. *P(s)* may be further denoted as:

$$\begin{bmatrix} Z_1 \\ Z_2 \\ Z_3 \\ e \end{bmatrix} = \begin{bmatrix} W_s & -W_sG \\ 0 & W_{ks} \\ 0 & W_tG \\ I & -G \end{bmatrix} \tag{10}$$

$$P = \begin{bmatrix} W_s & -W_sG \\ 0 & W_{ks} \\ 0 & W_tG \\ I & -G \end{bmatrix} = \begin{bmatrix} A & B_1 & B_2 \\ C_1 & D_{11} & D_{12} \\ C_2 & D_{21} & D_{22} \end{bmatrix} \tag{11}$$

From Eq. (10) and Eq. (11), the mixed sensitivity function can be written as:

$$P = \begin{bmatrix} W_sS \\ W_{ks}KS \\ W_tT \end{bmatrix} \tag{12}$$

Finding a rational function controller *K(s)* to solve a mixed sensitivity problem and stabilizing the CL system while meeting the following equation:

$$min\|P\| = min \begin{bmatrix} W_sS \\ W_{ks}KS \\ W_tT \end{bmatrix} \tag{13}$$

where P is the TF from input W to output Z. By applying the minimum gain theorem, change the H∞ to be the norm of $|T_{WZ}|$ less than unity, therefore,

$$min\|T_{WZ}\| = min\begin{bmatrix} W_s S \\ W_{ks} KS \\ W_t T \end{bmatrix} < 1 \quad (14)$$

Consequently, we can create a stabilizing controller. The algebraic Riccati equations must be solved to obtain $K(s)$, which minimizes the cost function. The robust control theory indicates that choosing two weight functions is necessary for the controller's synthesis. For choosing weights, there are several approaches described in the literature. The H∞ controller is then synthesized using the loop shaping methodology in most of these design methods, and the weighting functions are chosen by trial and error.
However, a trial-and-error method could not result in a stabilizing controller, which is the fundamental disadvantage of this kind of synthesis. The tuning parameters are the weights, and it usually takes multiple iterations to achieve weights, resulting in a satisfactory controller. Having stated that, a smart first step is to choose:

$$W_s = \frac{s/M + \omega_o}{s + \omega_o A} \quad (15)$$

$$W_{ks} = constant \quad (16)$$

$$W_t = \frac{s + \omega_o/M}{As + \omega_o} \quad (17)$$

The value of A should be less than one for maximum steady state equipoise ($A = 0.01$), ω_o defines as desired bandwidth, and M is the sensitivity peak ($M = 2$). The $1/Ws$ is an upper bound on the desired sensitivity loop shape, and W_{ks}^{-1} will affect the controller output u which is identical to Ws boundary to the line $\omega = \omega_o$.
The values of $A = 0.01 (= -40dB)$, $M = 2 (= 6dB)$ and $\omega_o = 1$rad/sec.
To test the H∞ controller design process, a Plant-derived as:

$$Plant = \frac{39}{25s^2 + 7s - 4e005}$$

With the weight functions as,

$$Ws \text{ or } W_1 = \frac{s+300}{3s+15}; W_t \text{ or } W_3 = \frac{s+100}{s+200}$$

Solving the given plant, as a model shown in **Fig. 3**, we obtained the controller as,

$$K(s) = \frac{7.4325e11\ (s + 200)\ (s + 12.79)\ (s + 10.86}{(s + 4.027e04)\ (s + 1e04)\ (s + 1896)\ (s + 5)}$$

With ϒ = 0.6398, where ϒ is the robustness index

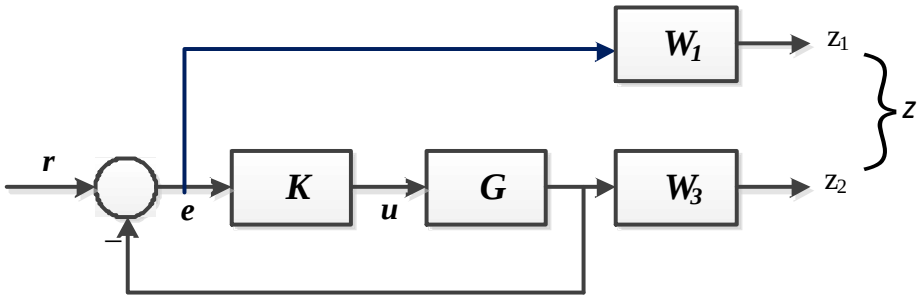

Figure 3. Mixed sensitivity H∞.

The CL system and open-loop singular values are shown in **Figs. 4**, **5,** and **6,** respectively. The $1/W_1$ and $1/W_3$ constraints and the singular values of S and T are shown in **Figs. 4** and **5,** respectively. The $1/W_1$ constraint is considered the performance boundary region for the designed controller, as shown in **Fig. 4**, and $1/W_3$ constraint is the boundary region of robustness for the designed controller, as shown in **Fig. 5**. It can be seen that the maximum singular values of S and T are both below the magnitude response of $1/W_1$ and $1/W_3$, respectively. This indicates that the performance and robustness specifications outlined by the weighting functions W_1 and W_3 are met. **Fig. 6** depicts the open-loop system (L)'s singular values concerning the performance constraint W_1 and robustness bound $1/W_3$. The lowest singular value of L is above the bound W_1 in the low-frequency band, while the greatest singular value of L is below the bound $1/W_3$ in the high-frequency range as a consequence of meeting performance and robustness criteria.

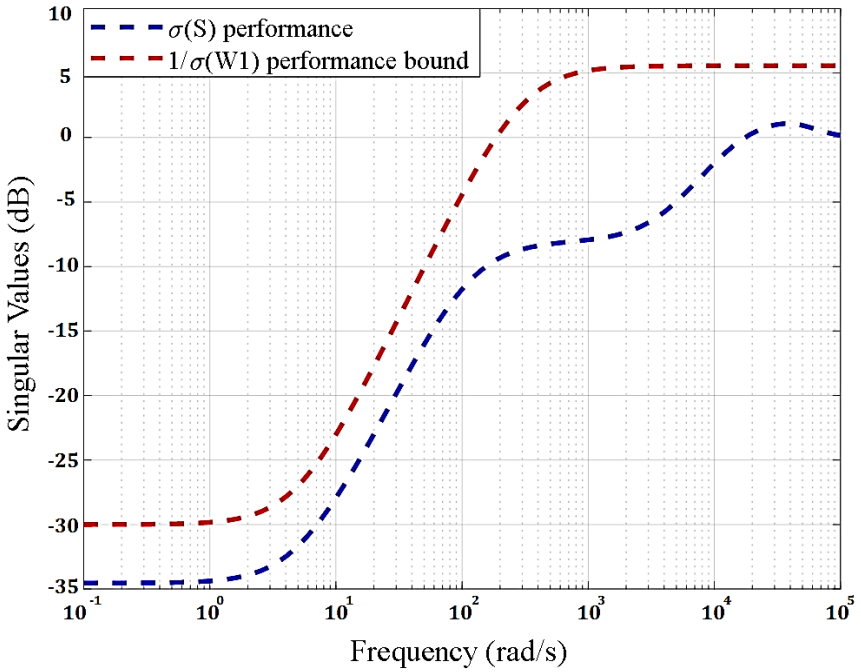

Figure 4. Singular values for the CLS performance achievement.

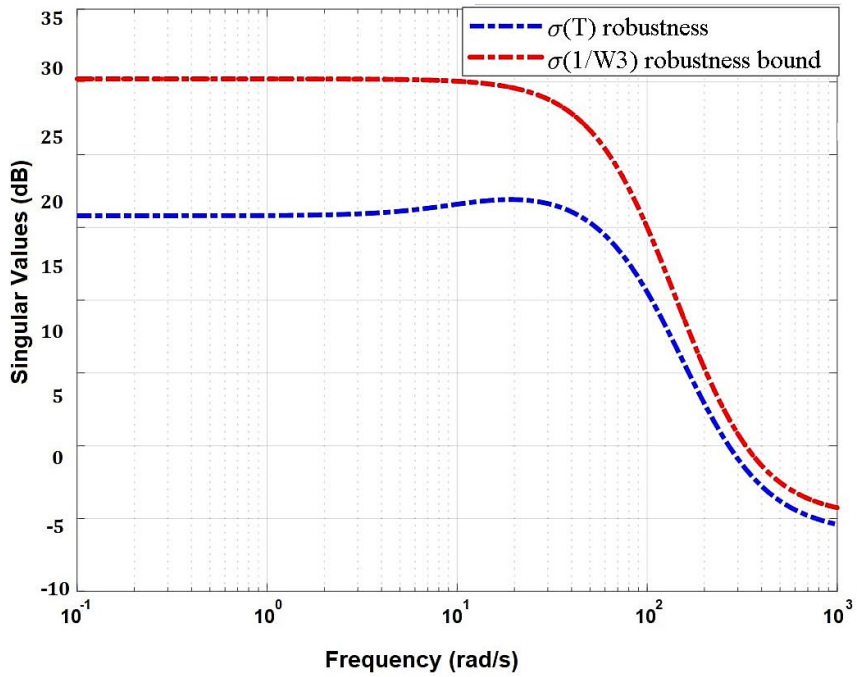

Figure 5. Singular values for the CLS robustness achievement.

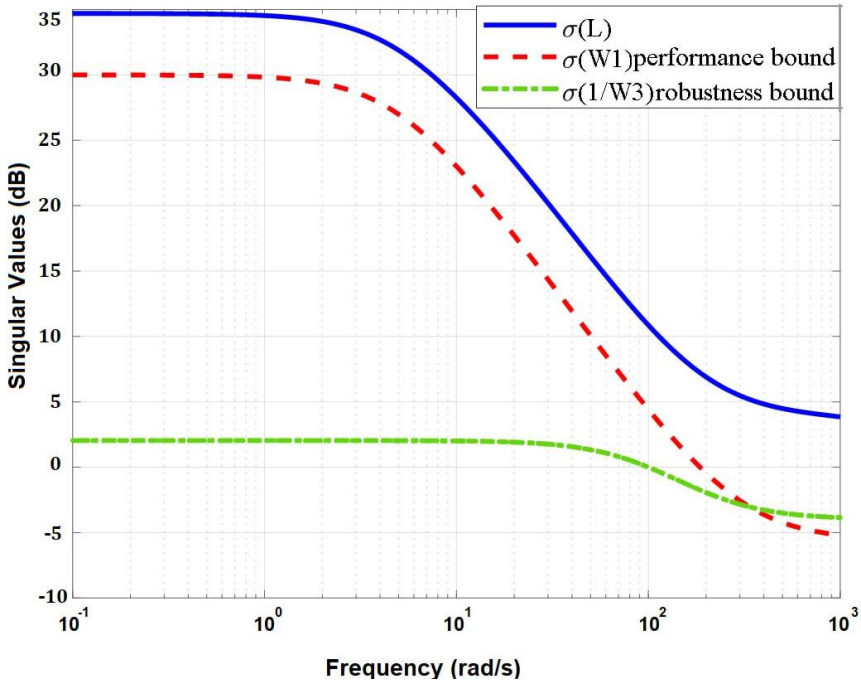

Figure 6. Singular values for the open-loop system.

4. H2 CONTROL

The H2 controller design method extends the LQG design approach, which may create a state space controller. In **(Khayat et al., 2017; Szabolcsi, 2018)**, the design procedure and solution of the H2 controller design problem are presented. The generalization of the LQG issue to the 'standard problem' and the elimination of random interpretations are well

known. The CL control system's standard setup can be seen in **Fig. 7**. Generally, the H2 norm of a TF, *G*, is its maximum value over the complete spectrum and is represented as the square of the second norm of the CL control system stable transfer matrix T_{zw}.

$$\|T_{zw}\|_2^2 = \frac{1}{2\pi} \underset{min}{tr} \int_{-\infty}^{+\infty} T_{zw}(-j\omega) T_{zw}(j\omega) d\omega \quad (18)$$

For further discussion, it is assumed that the plant dynamics p(s) is described with the state space representation elaborated in (6), and the plant dynamics p(s) are represented in (8).
The goal of the H2-optimization method was to meet the following criteria: closed-loop system stability, CL dynamic performance, and CL system robustness. To concurrently meet the above-described system characteristics, the controller must guarantee the following criteria: at low and high frequencies, the controller should achieve large and small open loop gains, respectively, and should stay far from the critical point of *-1+ 0j* at the crossover frequencies.
A Numerical Example for the Unmanned aerial vehicles flights UAV H2 Optimal Control System Design. There is a wider variety of unmanned aircraft systems (UAS) available. It is feasible to access the application's potential on a larger scale. As a component of the UAS, the UAV is getting increasingly complicated. The automatic flight control system, often known as the autopilot, must be installed within the UAV to assure flight safety that is at least as good as that of human aircraft. MIMO or the SISO approach can be used to represent the spatial mobility of a UAV. The Boomerang 60 small UAV is addressed, and a multi-input, multi-output dynamical model is studied **(Szabolcsi, 2018)**:
The TF of the Boomerang 60 UAV is given below:

$$Y(s) = \frac{-p(s)}{-\delta_a(s)} = \frac{A}{1+sT} = \frac{23.8289}{s+19.9149} \quad (19)$$

where A=1.1895, and T=0.04902
The roll rate stability augmentation mechanism frequently functions as an internal loop in the roll angle stabilization of the UAV, as seen in **Fig. 8**. The plant equations represent the UAV transfer equation in Eq. (20).

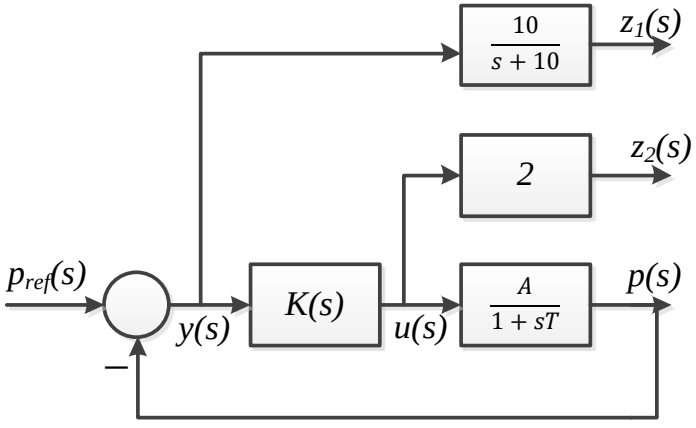

Figure 7. UAV's roll rate stability augmentation mechanism.

$$\left.\begin{array}{c} p_{ref} = w \\ p = x_1 \\ x_2 = 0.1 \rightarrow z_1 = 10x_2 \\ \dot{x}_1 = -\frac{1}{T}x_1 + \frac{A}{T}u \\ \dot{x}_2 = -x_1 - 10x_2 + w \\ z_2 = 2u \\ y = -x_1 + w \end{array}\right\} \quad (20)$$

Using Eq. (20) of the plant space state representation matrices, which are described by Eq. (9), can be derived as follows:

$$\mathrm{A} = \begin{bmatrix} -\frac{1}{\mathrm{T}} & 0 \\ -1 & -10 \end{bmatrix};$$

$$B_1 = \begin{bmatrix} 0 \\ 1 \end{bmatrix};\ B_2 = \begin{bmatrix} \frac{A}{T} \\ 1 \end{bmatrix};$$

$$C_1 = \begin{bmatrix} 0 & 10 \\ 0 & 0 \end{bmatrix};\ \mathrm{C}_2 = [-1 \quad 0];$$

$$D_{11} = \begin{bmatrix} 0 \\ 0 \end{bmatrix};\ D_{12} = \begin{bmatrix} 0 \\ 2 \end{bmatrix};\ D_{21} = 1;\ D_{22} = 0$$

In solving the given plant, the two inputs-two outputs state space equations with the CL system. The model of the plant is obtained by using MATLAB codes:

$$G = \begin{bmatrix} \frac{10}{(\mathrm{s}+10)} & \frac{-238.35}{(\mathrm{s}+19.92)} \\ 0 & 2 \\ 1 & \frac{-23.835}{(\mathrm{s}+19.92)} \end{bmatrix}$$

The optimal H2 controller *K(s)* has been obtained using the *h2syn* function of the robust control toolbox as given in the below TF:

$$K = \frac{0.92794\ (\mathrm{s}+19.92)\text{^}2\ (\mathrm{s}+10)}{(\mathrm{s}+21)\ (\mathrm{s}+19.92)\ (\mathrm{s}+10)\text{^}2}$$

ϒ=2.1972

The step response of the plant system with roll rate stability is shown in **Fig. 8.** TF's UAV CL roll rate stability has a fast response to a unit step function in the roll rate. Applying the normalized step response gives no overshoot indicating that the complete CL control system is non-oscillatory. Although good performance can be observed from the time domain response, the obtained performance index ϒ is greater than one, which means that the controller has feasible robustness but is not optimum.

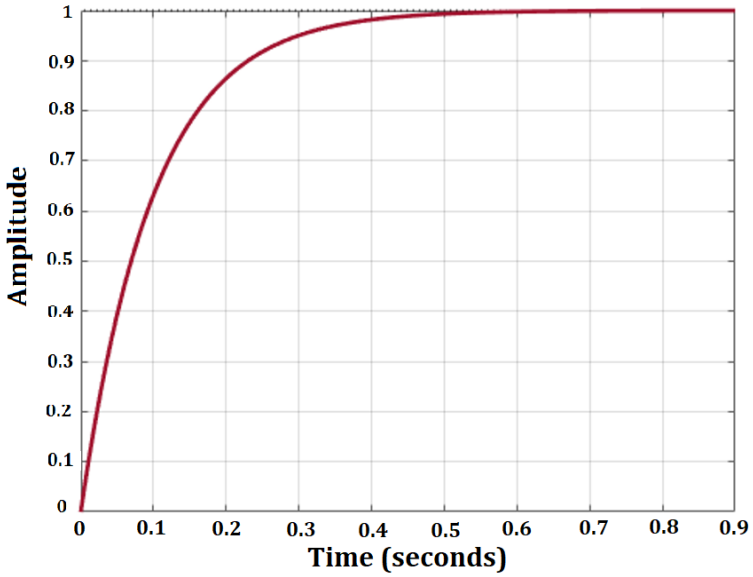

Figure 8. Step response of the plant UAV.

The previous UAV system is redesigned using the *hinfsyn* embedded function of MATLAB, yielding the H∞ controller *Ki(s)*:

$$Ki = \frac{3.4884\ (s+19.92)^2\ (s+10)}{(s+25.08)\ (s+19.92)\ (s+10)^2} \tag{21}$$

ϒ =0.8591

The obtained step response of the UAV plant is presented in **Fig. 9**. It can be noticed that the H∞ controller has a lower ϒ than the 4th-order controller. Since the obtained ϒ *is* lower than one, the obtained H∞ controller is more robust than the H2 controller. The outcomes of the H2 and H∞ designed controllers are summarized in **Table 1.**

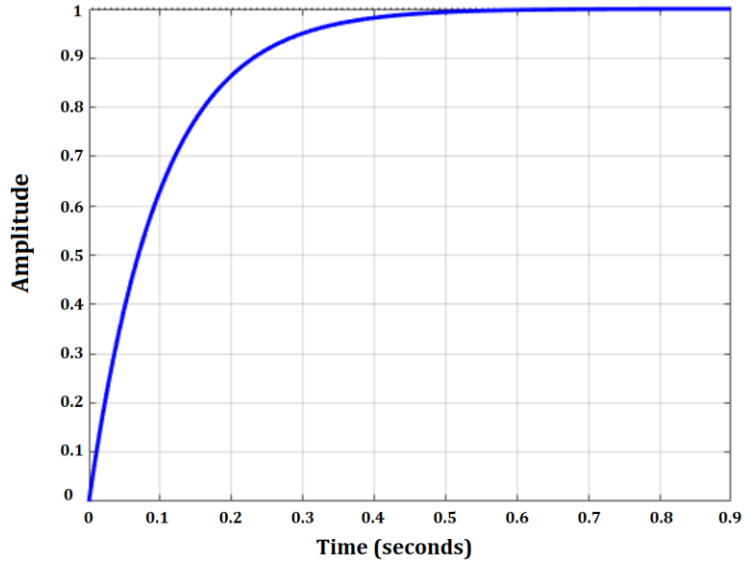

Figure 9. Step response of the UAV with K_i

Table 1. Features of the designed H2 and H∞ controllers

Control Strategy	Performance Index (γ)	Controller	Step Response	Pros and Cons
H2	2.1972	4th order	Fast and non-oscillatory	Achieves performance requirements but may not provide optimal robustness
H∞	0.8591	4th order	Fast and non-oscillatory	Ensures robustness and good performance but may not provide optimal performance

5. CONCLUSIONS

This paper introduces two methods for designing controllers and analyzing their behavior for unmanned aerial vehicles (UAV) and active suspension systems (ASS). These are the H∞ and H2 control design approaches. According to the results of the simulations, the selection of the controller is highly concerned with the system operations and uncertainties. The analysis generally emphasized that the H∞ controller ensures robustness, superior sensitivity performance, and high disturbance rejection, delivering great stability for any operating condition. In cases of multiple uncertainties and changing operational parameters, the H2 schemes are used intensively to guarantee stabilization and enhance the performance of the UAV. Finally, we concluded that choosing a proper robust controller depends on many parameters, such as the system behavior and the number of uncertainties due to their effects on the system's operation, to achieve the best performance and stability. Our future work will focus on the proposed controllers' order reduction, an attractive issue for industrial applications.

REFERENCES

Aghaie, Z., and Amirifar, R., 2007. H2 and H8 Controllers Design for an Active Suspension System via Riccati Equations and LMIs. In: *Second International Conference on Innovative Computing, Information and Control (ICICIC 2007)*. pp. 341–345. Doi:10.1109/ICICIC.2007.330

Araque, J.P.B., Zavoli, A., Trotta, D. and De Matteis, G., 2021. Genetic Algorithm Based Parameter Tuning for Robust Control of Launch Vehicle in Atmospheric Flight. *IEEE Access*, *9*, pp.108175-108189. Doi:10.1109/ACCESS.2021.3099006.

Bansal, A., and Sharma, V., 2013. Design and Analysis of Robust H-infinity Controller. *Control Theory and Informatics*, 3(2), pp. 7–14. https://iiste.org/Journals/index.php/CTI/article/view/6006

Gu, D.W., Petkov, P.H., and Konstantinov, M.M., 2005. . *Robust Control Design with MATLAB Advanced* Textbooks in Control and Signal Processing with Matla*b*, *Springer*.

Guessoum, H., Feraga, C., Mehennaoui, L., Moussa, S., and Lachouri, A., 2019. A robust performance enhancement of primary H∞ controller based on auto-selection of adjustable fractional weights: Application on a permanent magnet synchronous motor. *Transactions of the Institute of Measurement and Control*, 41, P.014233121882386. Doi:10.1177/0142331218823861.

Ibraheem, I.K., 2019. Anti-Disturbance Compensator Design for Unmanned Aerial Vehicle. *Journal of Engineering*, 26(1), pp. 86–103. Doi:10.31026/j.eng.2020.01.08.

Jafar, A., Rehman, S., Rehman, S., and Nisar, A., 2016. A Robust H infinity control law for unmanned aerial vehicle against atmospheric turbulence. Conference: 2nd IEEE International Conference on Robotics and Artificial Intelligence(ICRAI), 1-2 Nov., pp. 305–312. Doi:10.1109/ICRAI.2016.7791234.

Jiang, H., Wu, C., and Chen, B., 2022. Vibration Suppression of Hub Motor-Air Suspension Vehicle. *Energies*, 15(11), pp. 3916–3935. Doi:10.3390/en15113916.

Khayat, Y., Naderi, M., Shafiee, Q., Batmani, Y., Fathi, M., and Bevrani, H., 2017. Robust control of a DC-DC boost converter: H2 and H∞ techniques. In: *2017 8th Power Electronics, Drive Systems & Technologies Conference (PEDSTC)*. pp. 407–412. Doi:10.1109/PEDSTC.2017.7910360.

Lee, D.H., Joo, Y.H., and Tak, M.H., 2014. Periodically Time-Varying H∞ Memory Filter Design for Discrete-Time LTI Systems With Polytopic Uncertainty. *IEEE Transactions on Automatic Control*, 59(5), pp. 1380–1385. Doi:10.1109/TAC.2013.2289705.

Lee, M.-Y., Chen, B., Tsai, C.-Y., and Hwang, C.-L., 2021. Stochastic H∞ Robust Decentralized Tracking Control of Large-Scale Team Formation UAV Network System With Time-Varying Delay and Packet Dropout Under Interconnected Couplings and Wiener Fluctuations. *IEEE Access*, 9, pp. 41976-41997. Doi:10.1109/ACCESS.2021.3065127.

Li, T.-H.S., Tsai, S.-H., Lee, J.-Z., Hsiao, M.-Y., and Chao, C.-H., 2008. Robust H∞ Fuzzy Control for a Class of Uncertain Discrete Fuzzy Bilinear Systems. *IEEE Transactions on Systems, Man, and Cybernetics, Part B (Cybernetics)*, 38(2), pp. 510–527. Doi:10.1109/TSMCB.2007.914706.

Maccari, L.A., Montagner, V.F., Pinheiro, H., and Oliveira, R., 2012. Robust $\mathcal{H}2$ control applied to boost converters: Design, experimental validation and performance analysis. *Control Theory & Applications, IET*, 6, pp. 1881–1888. Doi:10.1049/iet-cta.2011.0755.

Mahmood, A., Kim, Y., and Park, J., 2014. Robust H∞ autopilot design for agile missile with time-varying parameters. *IEEE Transactions on Aerospace and Electronic Systems*, 50(4), pp. 3082–3089. Doi:10.1109/TAES.2014.130750.

Mehta, I., Garg, V., and Abraham, R.J., 2023. Design of a robust controller for a DC motor with structured uncertainties. *International Journal of Dynamics and Control*, 11(2), pp. 680–688. Doi:10.1007/s40435-022-01025-0.

Petersen, I.R., 2009. Robust H∞ Control of an Uncertain System Via a Stable Output Feedback Controller. *IEEE Transactions on Automatic Control*, 54(6), pp. 1418–1423. Doi:10.1109/TAC.2009.2017980.

Saud, L.J., and Hasan, A.F., 2018. Design of an Optimal Integral Backstepping Controller for a Quadcopter. *Journal of Engineering*, 24(5), pp. 46–65. Doi:10.31026/j.eng.2018.05.04.

Si, Y., Korada, N., Lei, Q., and Ayyanar, R., 2022. A Robust Controller Design Methodology Addressing Challenges Under System Uncertainty. *IEEE Open Journal of Power Electronics*, 3, pp. 402–418. Doi:10.1109/OJPEL.2022.3190254.

Sojoodi, M., and Majd, J. V., 2010. A technical approach to H2 and H∞ control of a flexible transmission system. In: *2010 IEEE Conference on Robotics, Automation and Mechatronics*. pp. 124–128. Doi:10.1109/RAMECH.2010.5513200.

Szabolcsi, R., 2018. Robust Control System Design for Small UAV Using H2-Optimization. *Land Forces Academy Review*, 23(2), pp. 151–159. Doi:10.2478/raft-2018-0018.

Vasičkaninová, A., and Bakošová, M., 2015. Robust controller design for a heat exchanger. In: *2015 20th International Conference on Process Control (PC)*. pp. 113–118. Doi:10.1109/PC.2015.7169947.

Wang, D., He, H., and Liu, D., 2017. Adaptive Critic Nonlinear Robust Control: A Survey. *IEEE Transactions on Cybernetics*, 47(10), pp. 3429–3451. Doi:10.1109/TCYB.2017.2712188.

Werner, H., 2006. Book review: Robust Control Design with Matlab, D.W. Gu., P.H. Petkov and M. M. Konstantinov. *Automatica*, pp.1619–1620.

Yaghi, M., and Önder Efe, M., 2020. H2/H∞ -Neural-Based FOPID Controller Applied for Radar-Guided Missile. *IEEE Transactions on Industrial Electronics*, 67(6), pp. 4806–4814. Doi:10.1109/TIE.2019.2927196.